

6.1 PROPERTIES OF SUPER-COOLED WATER CLOUDS OVER SOUTH POLE

Von P. Walden^{1*}, Mark E. Ellison¹,
Richard E. Brandt², Michael S. Town², Stephen R. Hudson², and Richard M. Jones³

¹University of Idaho, Moscow, Idaho

²University of Washington, Seattle, Washington

³Billings Senior High School, Billings, Montana

1. INTRODUCTION

The South Pole Atmospheric Radiation and Cloud Lidar Experiment (SPARCLE) was conducted at South Pole Station in the austral summer of 1999/2000 and throughout the full year of 2001 (Walden et al., 2001). In general, the goals of SPARCLE were to study climate processes related to longwave (infrared) radiation. Data from SPARCLE experiments have been used to investigate measurements of humidity, temperature, and pressure in the near-surface inversion layer (Hudson et al., 2004) and to build climatologies of the spectral downwelling longwave radiation and cloud fraction (Town et al., 2004; Town et al., 2005, this issue). Additional studies are still in-progress to investigate the spectral longwave emissivity and skin temperature of the surface and the temperature dependence of the foreign-broadened water vapor continuum, and to produce a one-year climatology of cloud microphysical properties over South Pole.

In addition, we are studying the properties of super-cooled water clouds at temperatures near -30 C. The different types and properties of clouds over Antarctica have a large effect on the radiation budget, which, in turn, can affect the general circulation of the atmosphere (Lubin et al., 1998). During the two summer field seasons of SPARCLE, water-only clouds were observed at times over South Pole. It is important to understand how often water clouds exist over Antarctica and how their microphysical properties differ from ice clouds. This is because clouds composed of water droplets interact differently with solar and infrared radiation than do clouds containing ice particles (or mixed-phased clouds). This paper describes the properties of super-cooled water clouds observed over South Pole Station in 2001.

* Corresponding author address: Von P. Walden, University of Idaho, Department of Geography, Moscow, ID 83844-3021
e-mail: vonw@uidaho.edu

2. INSTRUMENTATION

During SPARCLE, in-situ measurements of cloud particles were made using a hydrometeor videonode (HYVIS) (Murakami and Matsuo, 1990; Orikasa and Murakami, 1997). Figure 1 shows a picture of the instrument. Two miniature video cameras with different magnifications (high; 7X and low; 0.33X) are housed in the white Styrofoam section of the instrument. The upper metal section contains a fan for drawing particles into the instrument through the small black orifice, visible on top of the instrument. A lamp (attached to the copper tube shown on the front of the instrument) shines into the orifice to illuminate a tape that is coated with silicone oil. Cloud particles are drawn into the instrument by the pressure difference created by the fan, impact and

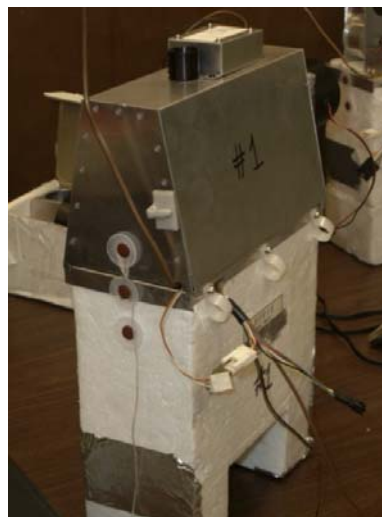


Figure 1. The hydrometeor videonode used during the South Pole Atmospheric and Cloud Lidar Experiment (SPARCLE) in 2001. The two video cameras are housed below in the white Styrofoam section. The silicone-coated tape and intake fan are housed in the upper metal part. The black intake orifice is visible on the top of the instrument.

stick to the coated tape, and are then photographed by the two video cameras in succession. The images were transmitted at 1.6 GHz to a receiver at the surface. A video cassette recorder (VCR) was attached to the receiver, which allowed storage of the images onto Hi8 video tapes. The Hi8 tapes were subsequently converted to digital video discs (DVDs) to facilitate image analysis on a computer workstation.

The HYVIS was operated both at the surface and aboard a tethered balloon (from AIR, Inc., Boulder, CO) in summer and a tethered kite in winter. (The HYVIS experiments conducted at the surface were designed to measure the sizes and shapes of diamond-dust ice crystals, but are not discussed here.) High winds and extremely low temperatures prevented the use of the balloon in wintertime. The tethered balloon and kite typically reach altitudes of 300 to 400 meters; the kite attained a maximum altitude of 1 km in winter.

A Vaisala RS-80 radiosonde was attached to the HYVIS to record the temperature and humidity as a function of pressure during the flight. The sonde was connected to a TMAX data acquisition board, which allowed transmission of data to a receiver at the surface at 403 MHz. A 2400-baud modem was connected to the receiver for storing the sonde data directly onto a personal computer.

3. MEASUREMENTS

Three flights using the HYVIS were flown in the austral summer of December 2000 and January 2001. Two flights were conducted in the austral autumn in February 2001. The duration of these flights ranged from 30 to 100 minutes with an average of about 60 minutes; the duration was limited primarily by the lifetime of the batteries used to power the HYVIS and the radiosonde.

Various types of clouds (ice, water, and mixed clouds) were sampled during these flights, but in this study, we concentrate on a section of a single flight from 2 February 2001 in which the HYVIS sampled only super-cooled water droplets within a low-lying cloud. The duration of this flight was 100 minutes. Sixty-six HYVIS images were processed from an 18-minute section of the flight.

Figure 2 shows examples of two high-magnification images from the HYVIS taken on 2 February 2001. The images were acquired about 6 minutes apart and indicate very different droplet sizes and concentrations.

Figure 3 shows time series of data from the Vaisala radiosonde taken during the tethered balloon flight. The surface pressure at South Pole during the time of flight was about 695 hPa. The

balloon attained a maximum altitude of about 450 meters, which corresponds to about 650 hPa. A temperature inversion is evident near the maximum altitude of the balloon (lowest pressure). The relative humidity with respect to water is generally between 90 and 100%. At these temperatures the relative humidity with respect to ice is super-saturated at values between about 120 and 130%. The vertical dashed lines in each panel of Figure 3 correspond to the approximate times that the images shown in Figure 2 were obtained.

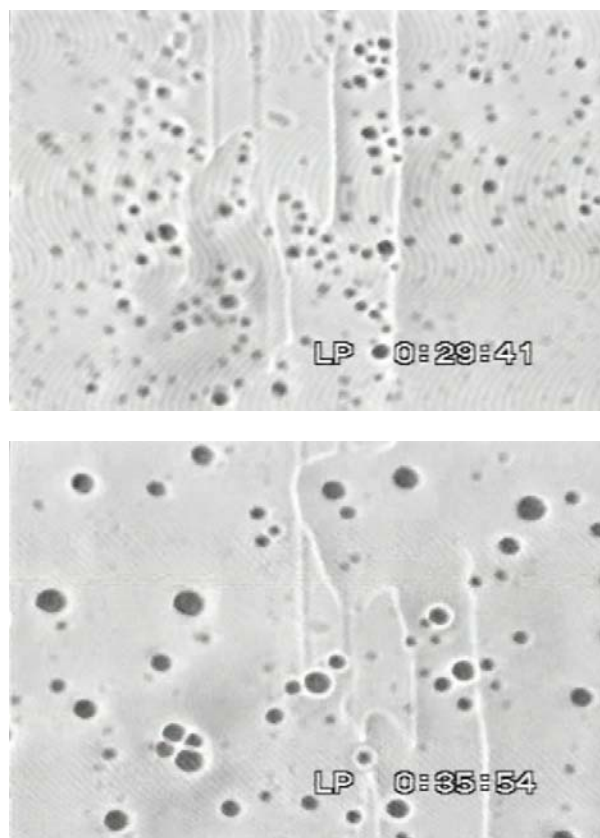


Figure 2. HYVIS images obtained on 2 February 2001 at South Pole Station. The round, black objects are super-cooled water droplets sampled from a cloud. The white lines are streaks in the silicon oil on the sampling tape. The times on the images are relative to about 0230 GMT on 2 February 2001.

4. IMAGE ANALYSIS

The DVD files were viewed using a television screen and a standard DVD player to visually identify times when super-cooled water droplets

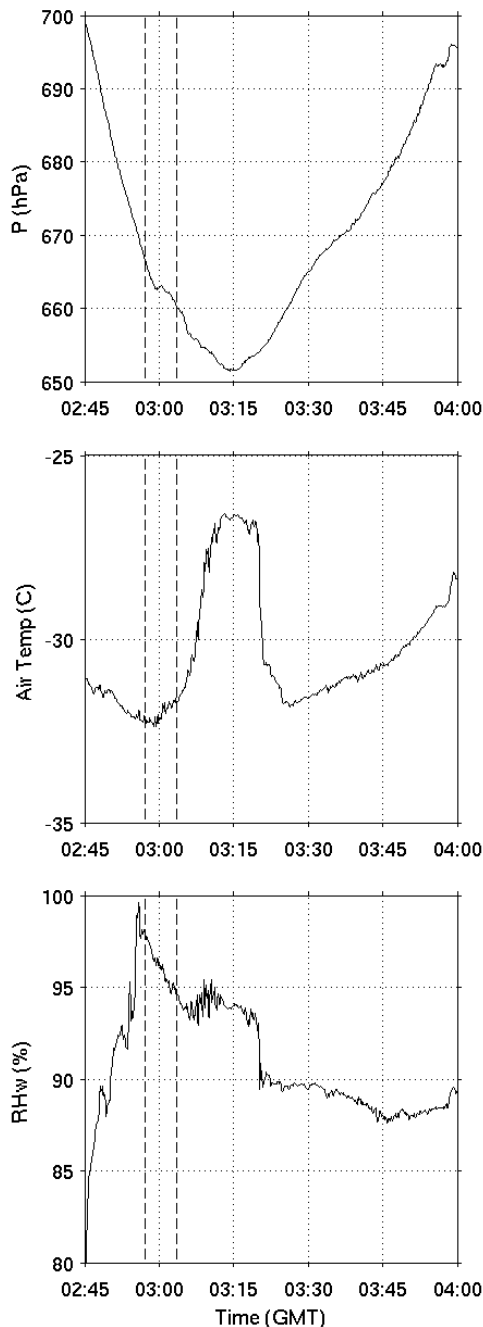


Figure 3. Time series plots of the Vaisala radiosonde data obtained during a tethered balloon flight on 2 February 2001 at South Pole Station. The upper panel shows the atmospheric pressure; the lowest pressure of 652 mb corresponds to about 450 meters above the surface (695 mb). The middle panel shows the temperature. The lower panel shows the relative humidity with respect to water. The vertical dashed lines indicate the approximate times that the images were taken in Figure 2.

were observed. These time segments were played back on an external Dae-woo DVD player and were then captured digitally with an Osprey-100 video capture card as raw Audio Video Interleaved (AVI) files (YUY2 color standard) at 10 frames per second (FPS). The raw AVI files were loaded into a professional video editing software package (Adobe Premiere Pro) and converted to series of still images, which were then stored as Tagged Image File Format (tiff) files. Within each AVI file, there are sequences of images in which the cameras on the HYVIS switch between low magnification and high magnification.

In this study, we are only concerned with images acquired with the high-magnification camera so all images obtained at low magnification are ignored. We use the final image in a series of images that were obtained just before the silicone-coated tape advanced; these final images are about 17 to 18 seconds apart.

The Image Processing Toolbox, available as part of the Matlab software package (The Mathworks, Natick, MA), was used to identify super-cooled water droplets in the HYVIS images. The essential step in identifying droplets is to properly determine what is the background of the image and, therefore, what are water droplets. This must be done frame-by-frame because the intensity of the background can change due to fluctuations in the illumination of the tape and in the thickness of the silicone oil on the tape. The background is determined using Otsu's method (Otsu, 1979) in Matlab. A binary image is then created where all pixels with values below the threshold are set to 255 (white) and those equal to and above the threshold are set to 0 (black). The Matlab software then identifies and labels all the black areas as objects with a variety of properties, including major and minor axes, centroid, eccentricity, and the total pixel area.

Figure 4 shows an image in which the droplets have been identified. The red circles indicate the boundaries around the super-cooled water droplets.

The major and minor axes of the objects are converted from pixels to micrometers using the image of 1-mm scale, shown in Figure 5. The conversion factor is about 2.6 μm per pixel.



Figure 4. HYVIS image showing areas that have been identified as super-cooled water droplets. The boundaries around the droplets are shown in red.

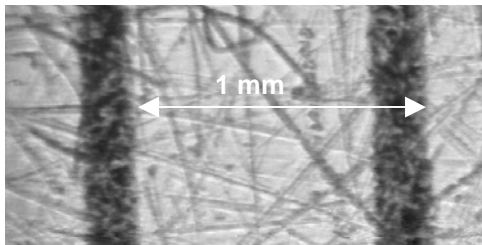


Figure 5. HYVIS image showing a ruler with 1-mm divisions under high magnification. This image is used to determine the conversion factor from pixels to micrometers.

5. SIZE DISTRIBUTIONS

Some of the objects identified by the Image Processing Toolbox are not actually water droplets. Sometimes dark portions of the background are selected. On occasion, very small, square objects that are only a few pixels across are selected. In addition, sometimes two water droplets impact near enough to each other on the silicone-coated tape that they appear connected, yielding an hourglass shape.

These anomalies are identified and eliminated from further analysis using the eccentricity of the objects, ϵ . Figure 6 shows a histogram of the eccentricities for over 6000 objects found in the sixty-six images considered here. The eccentricity is zero for a perfect circle and unity for a line. The objects with eccentricities of exactly zero in Figure 6 are anomalies. All of these objects are very small with major axes less than about 5 micrometers. In addition, most of the objects with

$\epsilon > 0.8$ are anomalous. Many of these are actually dark, jagged lines within the background, which are most likely thick layers of silicone oil. The highly asymmetric objects with $\epsilon > 0.8$ come from all size bins.

Figure 6 also shows that most of the objects have eccentricities of around 0.55, which corresponds to objects whose major axis is about 20% larger than its minor axis. The peak in the distribution of eccentricities occurs because the objects are not exactly circular and because of

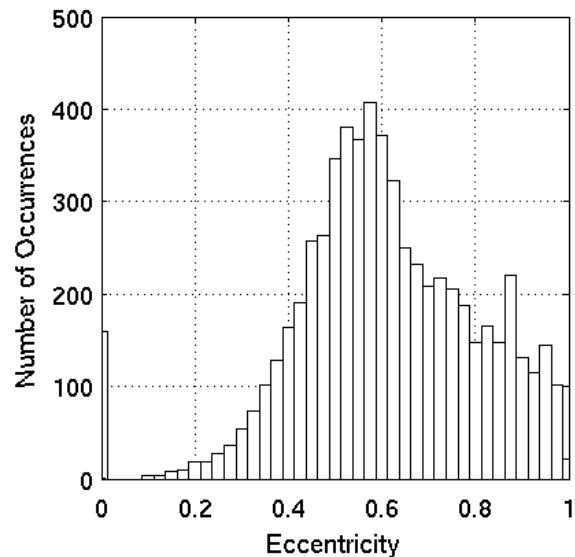


Figure 6. Eccentricity of “water droplet” objects derived from hydrometeor videosonde (HYVIS) images taken at South Pole Station on 2 February 2001. The objects with eccentricities of zero and greater than about 0.8 are anomalous features and are eliminated from further analysis.

how the Matlab software determines the centroid, and thus the major and minor axes, of each object.

The radii of the impacted water droplets are determined by taking the average of the major and minor axes, dividing these average diameters by two, and then converting the radii from pixels to micrometers using the conversion factor. Finally, the radii of the impacted water droplets are converted to radii of airborne droplets using a relationship determined in the laboratory at the National Center for Atmospheric Research (NCAR) after the field experiment (A. Hills and A. Heymsfield, personal communication, 2004). These laboratory tests photographed impacted water droplets from the side with a microscope, as the droplets lay in silicone oil on a microscope slide. The height and width (or diameter) for

various sizes of impacted droplets were then measured. By assuming the droplet shape on the microscope slide was that of a cosine, the volume of the water on the microscope slide was estimated. Since the volume of water on the slide is the same as what it would be in the atmosphere, a relationship between the impacted diameter of the droplets and its airborne diameter can be determined. The laboratory experiments show that the airborne water droplet radius r_a is related to the radius of impacted droplets r_i by

$$r_a = 0.486 * r_i.$$

Figure 7 shows a size distribution of the radii of airborne, super-cooled water droplets. The mode radius is about 7 micrometers. The fall-off at small radii may be influenced somewhat by the collection efficiency of the HYVIS, which has not yet been factored into this analysis. However, the size distribution shows a range of droplet radii from about 2 to 20 micrometers.

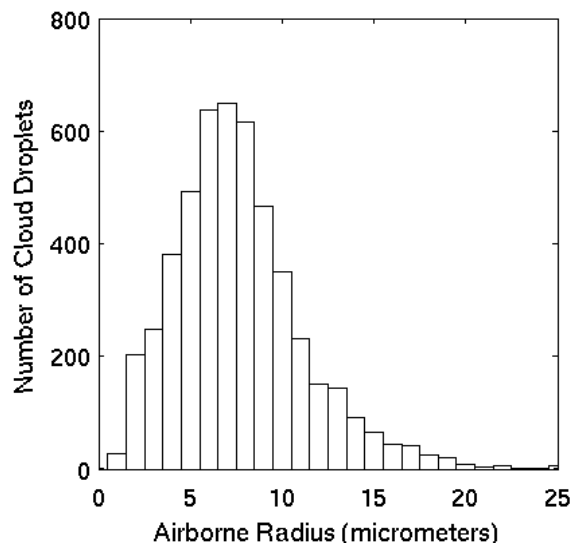


Figure 7. Size distribution of radii of super-cooled water droplets measured at South Pole Station on 2 February 2001. The mode of the distribution is 7 micrometers.

6. CONCLUSIONS

Summertime clouds over South Pole Station can be composed entirely of super-cooled water droplets at temperatures as low as -30 C. In-situ measurements were made inside such clouds during the South Pole Atmospheric Radiation and Cloud Lidar Experiment (SPARCLE) in 2001.

Images obtained with a hydrometeor videosonde are analyzed and show that the sizes of super-cooled water droplets range from about 2 to 20 micrometers with a mode of about 7 micrometers. More HYVIS images of water clouds obtained during SPARCLE will be analyzed in the future. The SPARCLE dataset may allow the temporal and altitudinal variation to be determined of droplets within some of the water clouds.

7. ACKNOWLEDGMENTS

Andy Heymsfield of NCAR contributed significantly to this project by lending us two hydrometeor videosondes and receiving equipment for SPARCLE. Hal Cole of NCAR provide use of a 403-MHz receiver that was used to acquire data from the Vaisala radiosondes. Alan Hills of NCAR (with assistance from Andy Heymsfield) performed essential laboratory tests to characterize the hydrometeor videosondes. This research was supported by NSF grants OPP-02-30114 to the University of Idaho, OPP-97-26676 and OPP-02-30466 to the University of Washington, plus a supplemental grant from the Teacher's Experiencing Antarctica (TEA) project through NSF's Office of Polar Programs.

8. REFERENCES

- Hudson, S.R., M.S. Town, V.P. Walden, and S.G. Warren, 2004: Temperature, humidity, and pressure response of radiosondes at low temperatures. *J. Atmos. Ocean. Tech.*, **21**, 825-836.
- Lubin, D., B. Chen, D.H. Bromwich, R.C.J. Somerville, W.-H. Lee, and K.M. Hines, 1998: The impact of antarctic cloud radiative properties on a GCM climate simulation, *J. Climate*, **11**, 447-462.
- Murakami, M., and T. Matsuo, 1990: Development of the hydrometeor videosonde. *J. Atmos. Ocean. Tech.*, **7**, 613-620.
- Orikasa, N., and M. Murakami, 1997: A new version of hydrometeor videosonde for cirrus cloud observations. *J. Meteor. Soc. Japan*, **75**, 1033-1039.
- Otsu, N., 1979: A thresholding selection method from gray-level histogram. *IEEE Transactions on Systems, Man, and Cybernetics*, **9**(1): 62-66.

Town, M.S., V.P. Walden, and S.G. Warren, 2004: Spectral and broadband longwave downwelling radiative fluxes, cloud radiative forcing and fractional cloud cover over the East Antarctic Plateau, submitted to *J. Climate*, 2004.

Town, M.S., V.P. Walden, and S.G. Warren, 2004: Cloud cover climatology for the South Pole from surface-based infrared radiation measurements, in *Proc. 8th Conf. Polar Meteorology and Oceanography*, San Diego, CA, this issue.

Walden, V.P., S.G. Warren, J.D. Spinhirne, A. Heymsfield, R.E. Brandt, P. Rowe, M.S. Town, S. Hudson, and R. M. Jones, 2001: The South Pole Atmospheric Radiation and Cloud Lidar Experiment (SPARCLE), in *Proc. 6th Conf. Polar Meteorology and Oceanography*, San Diego, CA, pp. 297–299.